Journal of Geotechnology and Energy | vol. 38 | no. 2 | 2021 | pp. 25–38

https://doi.org/10.7494/jge.2021.38.2.25

Paweł Zyzański

AGH University of Science and Technology
ORCID: 0000-0003-0248-7513

PERFORMANCE ANALYSIS OF A HORIZONTAL WELL LOCATED IN AN UNDERGROUND GAS STORAGE FACILITY

Date of submission:
28.06.2021

Date of acceptance:
29.06.2021

Date of publication:
31.08.2021

© 2021 Author. This is an open access publication, which can be used, distributed, and reproduced in any medium according to the Creative Commons CC-BY 4.0 License

https://journals.agh.edu.pl/jge

Abstract: Natural gas is the most ecological fossil fuel thanks to lower CO_2 emissions and no dust pollution, hence it is included into raw materials beneficial from the point of view of environmental protection. Natural gas is extracted from deposits often located at great depths by means of both vertical and horizontal drilling, characterised by high efficiency in terms of obtaining the highest possible productivity, which will allow the existing resources of the deposit to be exploited in the shortest possible time.

The paper analyses the influence of factors such as reservoir pressure, the thickness of the reservoir, the length of a horizontal section, average permeability of a reservoir, turbulence coefficient and water exponent on the process of lifting a liquid phase during the operation of a horizontal well located in an underground gas storage facility.

The calculations were carried out using data concerning exploitation of the "B" natural gas field and conducted using the "IHS PERFORM" computer programme, which is the leading industry software for carrying out analyses of productivity changes in gas wells.

In the final part of the article, conclusions are given, summarising the results of the nodal analysis reservoir performance curve (IPR) and well throughput curve (VLP).

Keywords: horizontal well, IPR, VLP, gas rate, UGS facility

1. Introduction

Energy raw materials, especially environmentally friendly raw materials, are becoming increasingly important and include the natural gas known as “blue fuel”. Natural gas is extracted from deposits often located at great depths by means of both vertical and horizontal drilling.

It is important that both vertical and horizontal wells are characterised by high efficiency in terms of obtaining the highest possible productivity, which will allow the existing resources of the deposit to be exploited in the shortest possible time.

The paper analyses the influence of factors such as reservoir pressure, the thickness of the reservoir, the length of a horizontal section, average permeability of a reservoir, turbulence coefficient and water exponent on the process of lifting a liquid phase during the operation of a horizontal well. The calculations were carried out using data concerning exploitation of the “B” natural gas field and conducted using the “IHS PERFORM” computer programme, which is the leading industry software for carrying out analyses of productivity changes in gas wells. The following correlations were used in the horizontal well performance analysis:

- Joshi’s correlation for calculating productivity for a horizontal well,
- the Hagedorn & Brown correlation for determining the course of pressures in a well for two-phase flow,
- the Lee, Gonzalez & Eakin correlation for calculating changes in gas viscosity,
- the Dranchuk & Purvis – Robinson correlation for calculation of deviation factor of real gas z.

The results of the calculations are presented in the form of graphs. In the final part of the article, conclusions are given, summarising the results of the analysis. In the further part of the article, the author focused on the course of operation of a horizontal well located in an underground gas storage facility.

2. Method section

2.1. A brief description of the underground gas storage facility “B”

The Underground Gas Storage Facility (UGS) is located in the partially depleted “B” natural gas field. This field is geologically located in the central part of the pre-Sudetic monocline in the northern edge of Carboniferous tectonic element called the Wolsztyn Dike. The structure of the “B” gas field is formed by a reef in the Zechstein limestone developed on a “paleovoltage” in the Zechstein basement . In the geological section of the reef of the “B” deposit 87.5 m of Zechstein limestone profile was found, developed in the form of permeable and porous rocks . The “B” gas field is massive and stratified with an area of about 1.53 km^2, with a volumetric energy system [1].

Petrophysical and technological parameters characteristic of the “B” PMG are summarised in Table 1. These parameters were obtained from the B3H well.

Table 1. Summary of parameters and data used in the analysis of the effectiveness of operation of the B3H well [2–4]

Parameters for PMG “B” [2]							
Total field resources [million nm^3]	Extracted field resources [million nm^3]	Buffer gas [million nm^3]	Reservoir pressure [MPa]	Reservoir temperature [K]	Average reservoir thickness [m]	Skin effect [–]	Coefficient deviation of gas z [–]
1110	546.367	563.633	18.3	371.15	29	2	0.968

Parameters of reef formations in PMG “B” [2]					
Average effective porosity [%]	Average horizontal permeability of deposit [mD]	Water saturation [%]	Average vertical permeability [mD]	Average clayey [%]	Hydrocarbon content in limestone profile [%]
14.98	59	14	19	8.14	81.33

Data of fluids taken for the analysis of efficiency of the B3H well on the “B” PMG [3]						
Water exponent [m^3/million nm^3]	Density of condensate [g/cc]	Density of gas [–]	Density of water [g/cc]	Salinity of water [mg/l]	CO_2 content [%]	Nitrogen content [%]
5	0.832	0.643	1.07	92.710	0.2298	18.3038

Casing pipe parameters of horizontal section of B3H well [4]				Parameters of B3H well trajectory [4]		
Drilling depth [m]	Outer diameter [mm]	Inner diameter [mm]	Absolute roughness [mm]	Max. measured depth (MD) [m]	Max. vertical depth (TVD) [m]	Max. borehole angle [°]
2850	177.8	151.49	0.01651	2850	2489.9	90

2.2. Brief characteristics of the correlations used in the analysis of horizontal well efficiency

The following equation was used to develop a performance curve for a horizontal well Joshi's equation (1) for steady-state flow of a weakly compressible fluid in an anisotropic reservoir, without formation damage [5].

$$q = \frac{2\pi k_H h \Delta p}{B\mu \left\{ \ln \left[\frac{\left(a + \sqrt{a^2 - \left(\frac{L}{2} \right)^2} \right)}{\frac{L}{2}} \right] + \left(\frac{I_{ani} h}{L} \right) \ln \frac{I_{ani} h}{\left[r_w \left(I_{ani} + 1 \right) \right]} \right\}} \quad (1)$$

where:
q – borehole flow rate,
Δp – pressure difference [Pa],
B – volume factor of gas [–],
k_H – horizontal permeability [m^2],
h – depth of borehole [m],
μ_g – gas viscosity [Pa·s],
L – length of horizontal section of the well [m],
r_w – radius of the well [m],
a – half the length of the horizontal well interaction ellipsoid [m],
I_{ani} – medium anisotropy coefficient [–],
k_V – vertical permeability [m^2],
r_{eH} – radius of the horizontal well interaction range [m].

In Joshi's formula, the function PD(tD) for a horizontal well is proposed, consisting of two members:

- The first describes the horizontal flow and depends mainly on the length of the horizontal section (L). The length (L) affects the longer half-axis of the ellipsoid (a), which is expressed by equation:

$$a = \frac{L}{2} \left\{ 0.5 + \left[0.25 + \left(\frac{r_{eH}}{\frac{L}{2}} \right)^4 \right]^{0.5} \right\}^{0.5} \quad (2)$$

- The second term (3) describes the flow in a vertical plane taking into account the medium anisotropy coefficient I_{ani} expressed by the relation:

$$I_{ani} = \sqrt{\frac{k_H}{k_V}} \quad (3)$$

The natural gas volumetric coefficient B_g is expressed by the relation:

$$B_g = \frac{V_{p,T}}{V_{sc}} = \frac{P_n T_z z_z}{P_z T_n z_n} \quad (4)$$

where:
$V_{p,T}$ – the volume occupied by the gas at p, T (in particular under field conditions),
V_{sc} – volume occupied by gas at standard conditions,
B_g – volumetric factor of natural gas,
P_n – pressure at normal conditions,
T_z – reservoir temperature,
z_z – deviation factor of real gas under reservoir conditions,
P_n – reservoir pressure,
T_n – temperature under normal conditions,
z_n – deviation coefficient of real gas under normal conditions, assumed to be equal to 1.

Due to the possibility of the occurrence of two-phase flow in a well, the Hagedorn & Brown correlation was used for description, expressing the change of pressure gradients and frictional pressure losses occurring in a pipe in time [6]. This correlation has been derived in the Anglo-Saxon system of units and is not usually converted to the SI system for accuracy of calculations.

In this correlation, the energy conservation equation assuming $dWs = 0$ is written in the following form:

$$\frac{dp}{dz} = g\rho_{sr} + \frac{2 f_f w_m^2}{D} + \rho_{sr} \frac{\Delta \left(\frac{w_m^2}{2} \right)}{\Delta z} \quad (5)$$

The nature of flow in two-phase gas-liquid systems can be determined based on the use of charts, where the flow regime is a function of: flow rate of each phase, fluid properties and the diameter of the extraction pipes. To describe the flow character, dimensionless numbers are used: input fluid N_{vl} and input gas N_{vg}, internal diameter N_D and fluid viscosity N_μ defined respectively by the relations [7]:

$$N_{vl} = 1.938 V_{sl} \left(\frac{\rho_L}{\sigma} \right)^{\frac{1}{4}} \quad (6)$$

$$N_{vg} = 1.938 V_{sg} \left(\frac{\rho_L}{\sigma} \right)^{\frac{1}{4}} \quad (7)$$

$$N_D = 1.938 D \left(\frac{\rho_L}{\sigma} \right)^{\frac{1}{2}} \quad (8)$$

$$N = 1.938\mu_L \left(\frac{1}{\mu_L \sigma^3}\right)^{\frac{1}{4}} \tag{9}$$

where (for equations (5), (10) and (11)):

f_f – flow resistance coefficient,
w_m – velocity of the mixture of both phases,
ρ_{sr} – the average density of the flowing fluid expressed by the relation:

$$\rho_{sr} = (1 - \omega_l)\rho_g + \omega_l \rho_l \tag{10}$$

The mixture velocity w_m is the sum of the surface velocities of the phases:

$$w_m = w_{sc} + w_{sg} \tag{11}$$

In order to calculate the pressure drop in the wellbore from equation (5), the amount of "phase lag" for the fluid ω_l, and the flow resistance coefficient for the mixture f_f must be determined in advance. "Phase lag" of the fluid and the average density are determined from the graphs (Figs. 1–3) using the dimensionless numbers N_{vl} and N_{vg} previously defined by relations (6)–(9): N_D, N_μ.

"Phase delay" is determined from the graphs in (Figs. 1–3) by the following algorithm [7]:

- calculation of N_L,
- determination of the CN_L from (Fig. 1),
- calculation of the quotient (12):

$$\frac{N_{vl} p^{-1} (CN_L)}{N_{vg}^{0.575} p_a^{-1} N_D} \tag{12}$$

where:

p – pressure at the well interval for which the pressure gradient is calculated,
p_a – atmospheric pressure.

Determination of the quotient value based on Figure 2.

Calculation of the auxiliary quotient (13):

$$\frac{N_{vg} N_L^{0.380}}{N_D^{2.14}} \tag{13}$$

Determination of the value of the borehole slope correction Ψ (Fig. 3).

The magnitude of the "phase lag" ω_l is expressed by the formula:

$$\omega_l = \left(\frac{\omega_l}{\Psi}\right)\Psi \tag{14}$$

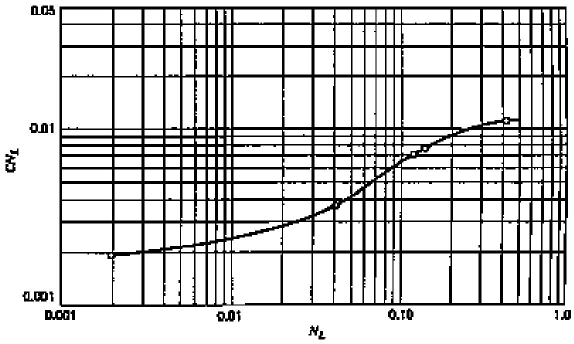

Fig. 1. Plot of CN_L dependence on N_L viscosity number [7]

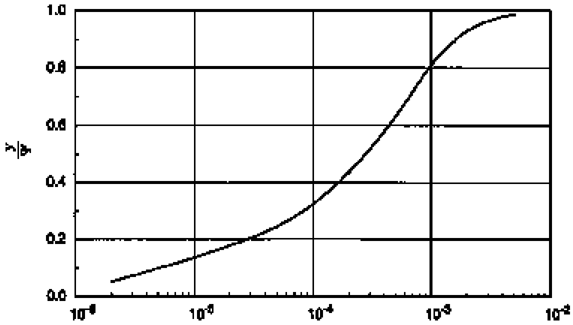

Fig. 2. Diagram of phase delay ω as a function of the product of $\frac{N_{vl} p^{-1} (CN_L)}{N_{vg}^{0.575} p_a^{-1} N_D}$

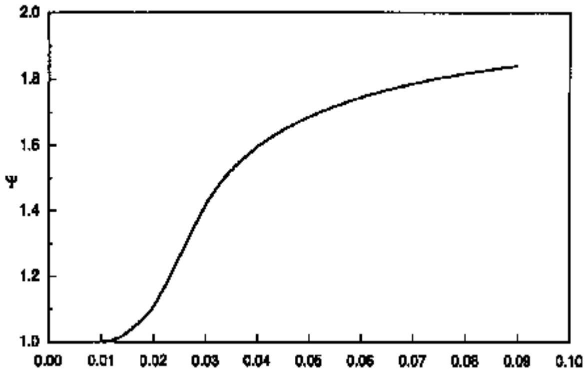

Fig. 3. Correction diagram Ψ as a function of the product of $\frac{N_{vg} N_L^{0.380}}{N_D^{2.14}}$

The density of the mixture is calculated from equation (13).

The determined density ρ_m is needed to calculate the hydrostatic pressure and the pressure loss due to friction.

Formula for hydrostatic pressure:

$$\Delta P_{HH} = \frac{\rho_m g \Delta z}{144 \rho_c} \tag{15}$$

The formula for pressure loss due to friction is of the form:

$$\Delta P_f = \frac{\rho_{NS} f V_m D}{\rho_m} \tag{16}$$

where:
D – pipe inside diameter [ft],
f – coefficient of friction [–],
g – gravitational acceleration [32.2 ft/s^2],
ΔP_{HH} – change in pressure [psi],
ΔP_f – pressure change due to friction [psi],
V_{sl} – fluid surface velocity [ft/s],
V_{sg} – gas surface velocity [ft/s],
V_m – mixture velocity [ft/s],
Δz – change in height [ft],
μ_L – viscosity of the liquid [cP],
ρ_L – density of liquid [lb/ft^3],
ρ_{NS} – density of the fluid in the slip region [lb/ft^3],
ρ_m – density of the mixture [lb/ft^3],
σ – surface tension at the gas/liquid interface [dynes/cm].

Before further use of the correlation, the author checked the ranges of its applicability.

Gas viscosity calculations were performed using the correlation of Lee, Gonzalez and Eakin, expressed by the formula [8]:

$$\mu_g = 10^{-4} K^{\left[X \rho_g{}^{Y}\right]} \tag{17}$$

where:
μ_g – gas viscosity [Pa·s],
ρ_g – density of gas in reservoir at specific pressure and temperature [kg/m^3].

Parameters K, X and Y are expressed by relations (18)–(20) [8]:

$$K = \frac{\left(0.00094 + 0.02 M_{wa}\right) T^{1.5}}{\left(209 + 19 M_{wa}\right)} \tag{18}$$

$$X = 3.5 + \frac{986}{T} + 0.01 M_{wa} \tag{19}$$

$$Y = 2.4 - 0.2X \tag{20}$$

where:
T – temperature of the reservoir [°C],
M_{wa} – substituted molecular weight of the gaseous mixture.

The dynamic viscosity of water was determined from the Matthews and Russell curve expressed by equation (21) [9]:

$$\mu_w = \left[\left(\frac{38.3}{T_f{}^{0.5}}\right) - \left(\frac{14.6}{T_f{}^{0.25}}\right) + 1.48\right]\left[1 + \left(\frac{C_{ds}}{300}\right)\right] \tag{21}$$

where:
μ_w – dynamic viscosity of water [0.001 Pa·s],
T_f – temperature [°C],
C_{ds} – concentration of dissolved solids.

The empirical correlation of Dranchuk–Purvis–Robinson (22) expressed by the relation was used to calculate the real gas deviation coefficient z:

$$q_r = \frac{0.27 p_{pr}}{z T_{pr}} \tag{22}$$

This correlation is valid in the ranges [9]:

$$1.05 < T_{pr} < 3.0 \quad \text{and} \quad 0.2 < P_{pr} < 3.0.$$

The q_r best value is calculated using the Benedict–Webb–Rubin equation of state.

3. Results

3.1. Analysis of the effectiveness of the B3H well

In an analysis of the effectiveness of the operation of the B3H well, the author, as mentioned above, took into account the following: the length of the horizontal section, which results from the technology used to drill the well; reservoir pressure; thickness of reservoir; average permeability of the reservoir; turbulence coefficient; and water exponent. These parameters, apart from the first one, are essentially beyond our control, as they are determined by the properties of the discovered reservoir.

Two characteristic curves for the operation of the reservoir and the well are shown in Figure 4. These are: the IPR (Inflow) curve, which represents the inflow of fluid from the reservoir to the well, and the VLP (Outflow) curve, which represents the throughput of the well. These curves intersect at a characteristic point, the abscissa of which, at a well-defined pressure depression, is the flow rate at which the well may be operated. In the case of a need to lift fluids out of the well, it is advisable to define limits to the well's flow rate at which this process occurs without problems. For this reason, two points are determined on the VLP curve with regard to maximum and minimum flow rates for proper flowing out of the well. In the diagram (Fig. 4), these points are marked as a green square indicating the minimum current flow rate capable of drawing off condensate and a blue triangle indicating the minimum current flow rate for drawing off water. In addition, the minimum current flow rate at which the unfavourable process of bed erosion occurs (bed scouring) is determined. The expenditures for these characteristic points: condensate removal, water removal and sand removal were determined on the basis of calculations carried out with the use of the IHS PERFORM computer program.

If the intersection of IPR and VLP curves is behind the green square, then there are conditions for transportation of condensate, at minimum expenditures and assumed initial factors used in the analysis, amounting for the B3H well to 339,246.4 m³/d. On the other hand, in cases where the intersection of the curves is beyond the blue triangle, conditions exist for rising water at minimum flow rate and assumed initial factors used in the analysis, amounting for the B3H well to 478,068.9 m³/d. The analysis also shows the flow rate causing erosion of the well with a pink dot. For the B3H well, this value is 2,662,138.6 m³/d, beyond which potential damage to the tubing in the well will occur.

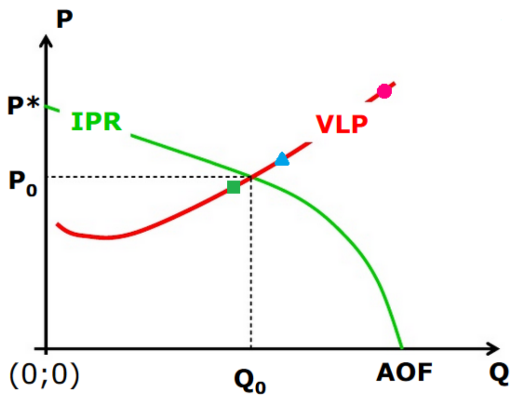

Fig. 4. Example of nodal analysis for a well [4], where: *IPR* – reservoir performance curve, *VLP* – well throughput curve, *P* – dynamic bottom pressure, P^* – reservoir pressure, P_0 – bottomhole pressure in the exploited B3H well, *Q* – flow rate, *AOF* – maximum potential flow rate, Green square – minimum current flow rate to remove condensate, blue triangle – minimum current flowrate for water removal, pink dot – erosion-inducing flow rate

Table 2. Summary of efficiency depending on individual B3H factors

Variant	Length of horizontal section [m]	Gas output [m³/d]	Variant	Average field permeability [mD]	Gas output [m³/d]
1	440	495,571	1	59	495,426
2	10	301,501	2	1	60,872.9
3	50	442,030	3	50	456,699
4	100	468,077	4	100	638,893
5	200	484,005	5	500	1,318,975
Variant	Reservoir pressure [kPa]	Gas output [m³/d]	Variant	Variant turbulence [1/m³/d]	Gas output [m³/d]
1	18,300	495,423	1	0.070629	495,431
2	16,500	271,320	2	0.035315	684,430
3	17,500	409,426	3	0.105944	408,126
4	19,000	561,896	4	0.141259	355,190
5	20,000	648,156	5	0.194231	304,328
Variant	Reservoir thickness [m]	Gas output [m³/d]	Variant	Water exponent [m³/million m³]	Gas output [m³/d]
1	29	495,010	1	5	495,571
2	10	293,196	2	0.001	495,670
3	20	413,473	3	50	390,285
4	50	641,797	4	100	386,819
5	150	1,051,710	5	150	344,094

3.2. Analysis of the efficiency of the B3H well as a function of the length of the horizontal section

Analysis of the graph of pressure vs. gas flow rate as a function of the length of the horizontal section (Fig. 5) shows that a change in this parameter produces significant differences in the results obtained. It is also noticeable that curves 1, 5 have the ability to carry condensate and water, while curves 3, 4 only carry condensate. Whereas curve 2 shows no drift of condensate. It is important that this parameter depends on the drilling, so you can manoeuvre this value in order to obtain the best expenditure. However, analysing the curve of the gas yield as a function of the length of the horizontal section (Fig. 6) it can be stated that in the range of the length of the horizontal section from 10 to 50 m the curve of the change of the yield from the length of the horizontal section increases significantly, which means that the gas yield also increases significantly. Further on, the curve from the value of the length of the horizontal section from 50 to 440 m flattens, which means that the gas flow rate will increase less and less. What is important here is the fact that after exceeding the above-mentioned value, the greater length of the horizontal section does not translate into an increase in gas output, but only generates greater costs.

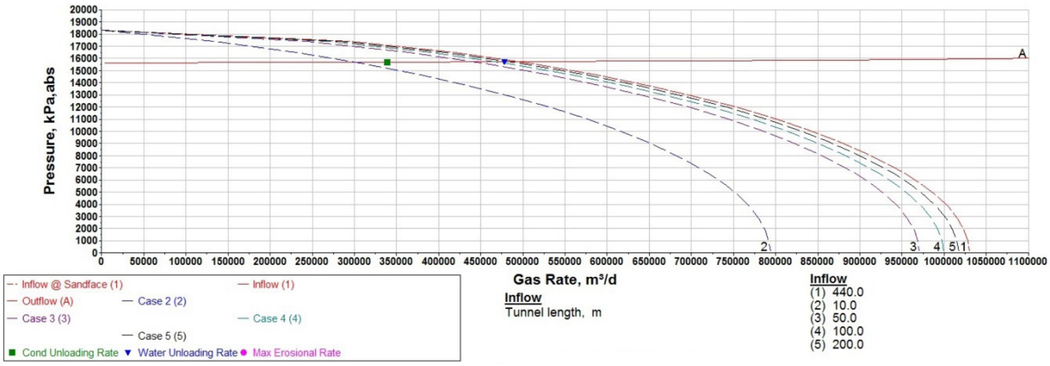

Fig. 5. Graph of pressure vs. gas flow as a function of the length of the horizontal section

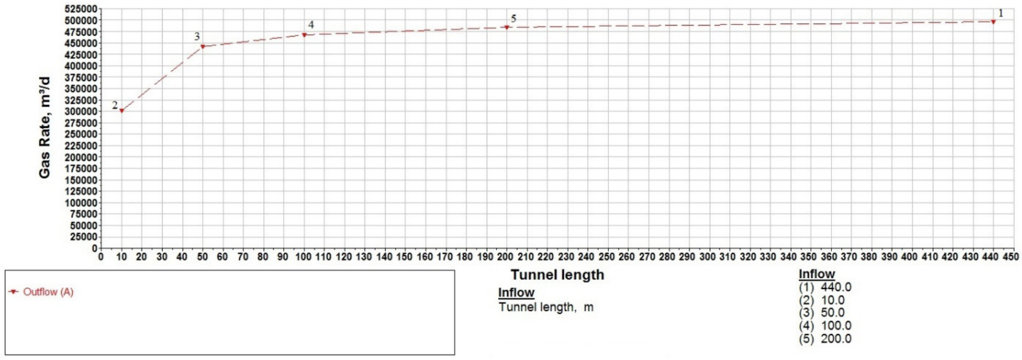

Fig. 6. Graph of gas flow rate vs. the length of the horizontal section

3.3. Analysis of the effectiveness of the B3H well in relation to reservoir pressure

By analysing the diagram of pressure vs. gas flow as a function of reservoir pressure (Fig. 7), it may be stated that this parameter is one of the most important ones which influence the effectiveness of well operation. It is also noticeable that for curves 1, 4 and 5, there is a possibility of taking out condensate and water, while for curve 3 – only condensate. On the other hand, in the case of curve 2, there is no drift of condensate. Analysing the diagram of gas flow in dependence on the pressure in the reservoir (Fig. 8) we can state that in the range of the pressure in the reservoir from 16,500 to 200,000 kPa, the curve of change of the flow in dependence on the pressure in the reservoir increases all the time, which means that the gas flow is also increasing. It is important here that this parameter is crucial in achieving higher gas flow rates in a well.

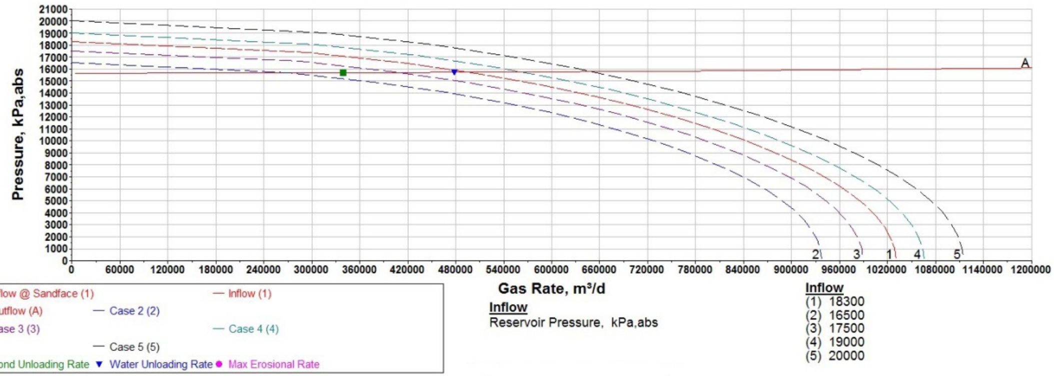

Fig. 7. Graph of pressure vs. gas flow rate as a function of pressure in the reservoir

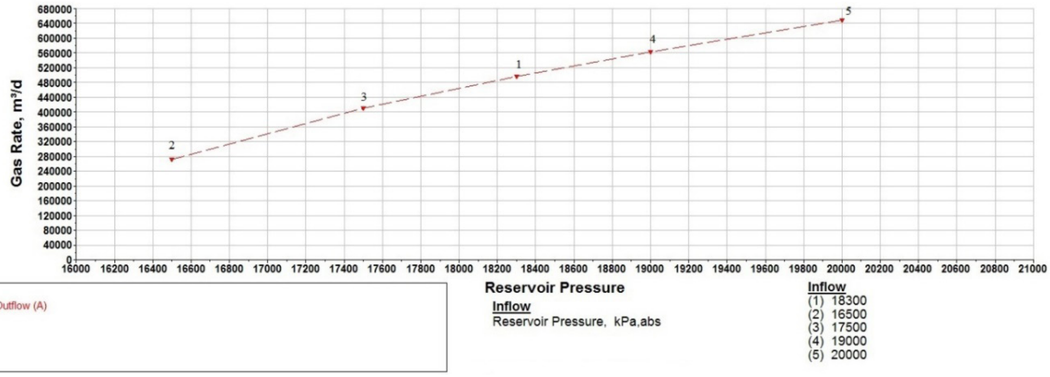

Fig. 8. Graph of gas flow rate vs. pressure in the reservoir

3.4. Analysis of effectiveness of the B3H well in relation to the thickness of reservoir

Analysis of the diagram of pressure vs. gas flow rate depending on the thickness of the reservoir (Fig. 9) shows that for curves 1, 4 and 5, there is a possibility of exporting condensate and water, whereas for curve 3 – only condensate. For curve 2, on the other hand, there is no drift of condensate. Analysing the diagram of gas flow in dependence on the reservoir thickness (Fig. 10) it can be stated that in the range of reservoir thickness from 10 to 150 m the curve of flow change from the reservoir thickness increases, which means that the gas flow also increases. The further course of the curve from the thickness of the reservoir from 50 to 150 m has a greater tendency to increase, which means that the gas flow rate will also increase to a greater extent.

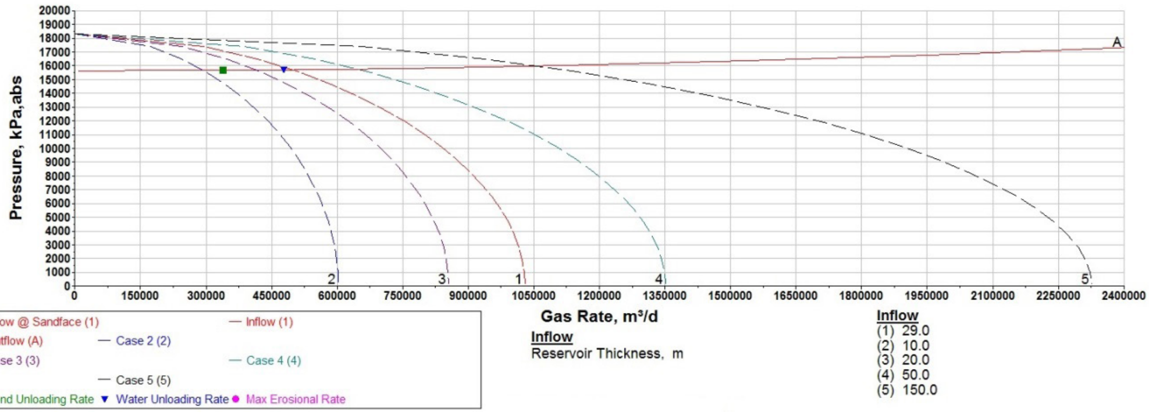

Fig. 9. Graph of pressure vs. gas flow rate as a function of reservoir thickness

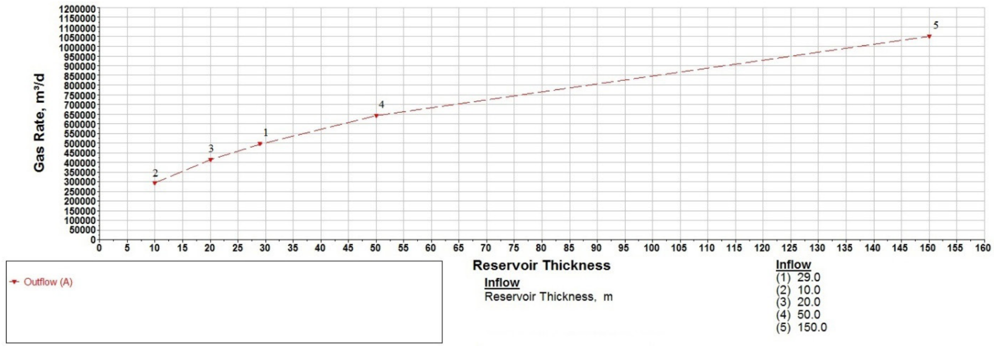

Fig. 10. Graph of gas flow rate vs. thickness of reservoir

3.5. Analysis of the effectiveness of the B3H well as a function of the average permeability of the reservoir

Analysing the diagram of pressure vs. gas flow as a function of the deposit average permeability (Fig. 11), it may be stated that in the interval of permability values from 0 to 60, the values of gas flow increase rapidly, while previously slower. It can also be seen that the IPR (Inflow) curve intersects the VLP (Outflow) curve behind the blue triangle, so for curves 1 and 4 to 5, it is possible to carry condensate and water out. For curve 3, only condensate outflow is possible.

Analysing the graph of the gas flow rate depending on the deposit average permeability (Fig. 12), it can be stated that in the range of the average permeability values from 1 to 50, the curve of the flow rate change from the permeability ratio increases, which means that the gas flow rate also increases. The further course of the curve from the value of the deposit average permeability from 100 to 500 grows more slowly, which means that the gas flow rate will increase less and less.

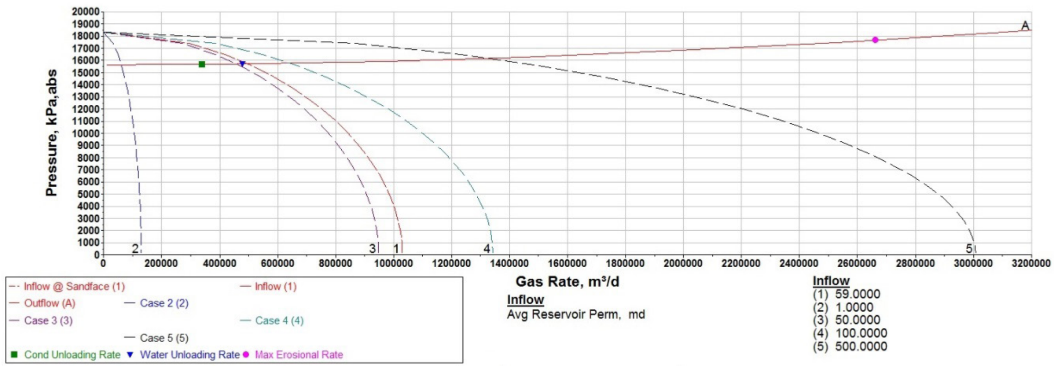

Fig. 11. Graph of pressure vs. gas flow rate as a function of the deposit average permeability

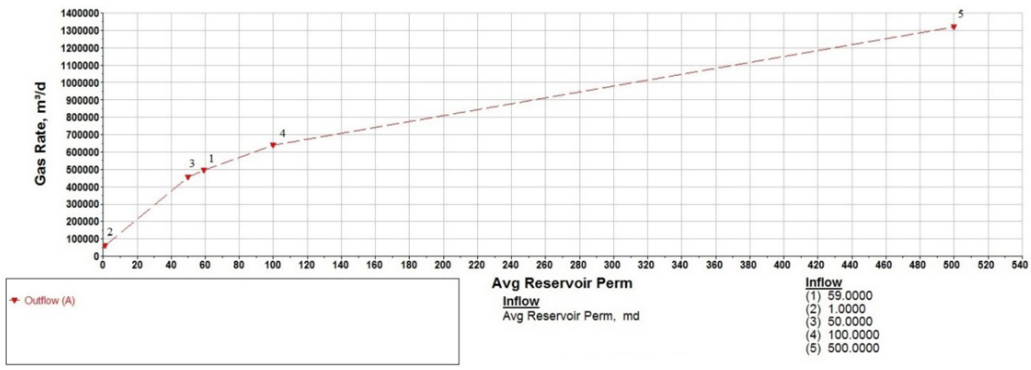

Fig. 12. Graph of pressure vs. gas flow rate as a function of deposit average permeability

3.6. Analysis of the efficiency of the B3H well as a function of turbulence ratio

By analysing the diagram of pressure versus gas flow rate as a function of the turbulence ratio (Fig. 13), it can be seen that the higher the turbulence ratio, the lower the gas flow rate. It is also evident that for curves 1 and 2, there is a possibility of removing condensate and water, for curves 3 and 4 – only condensate, whereas for curve 5 there is no possibility of removing both condensate and water. Additionally, this is the parameter on which the skin effect coefficient depends. Analysing the curve of the gas flow in dependence on the turbulence coefficient (Fig. 14) it can be stated that in the range of the turbulence coefficient value from 0.035315 1/m^3/d to 0.070629 1/m^3/d the curve of the flow change from the turbulence coefficient decreases strongly, which means that the gas flow also decreases significantly. The further course of the curve from the value of the turbulence coefficient 0.070629 1/m^3/d to 0.194231 1/m^3/d stabilises, which means that the gas flow rate will decrease less and less.

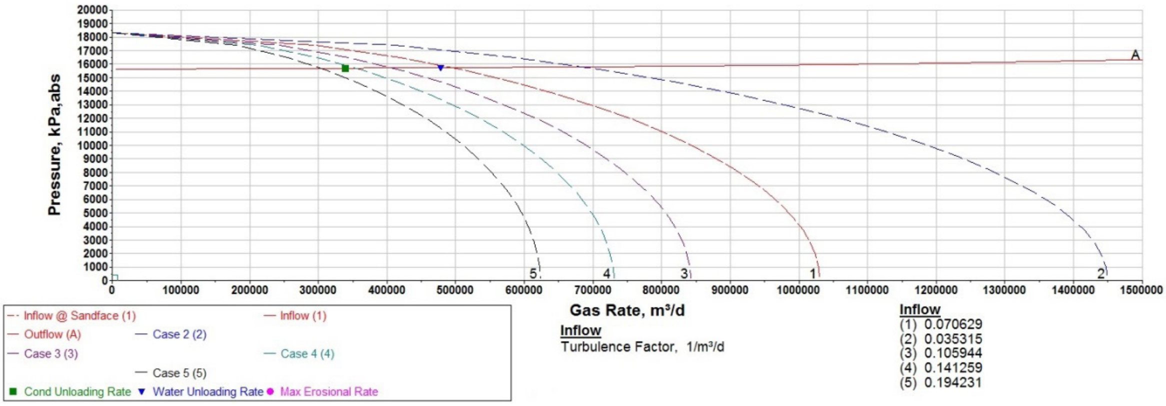

Fig. 13. Graph of pressure versus gas flow as a function of turbulence ratio

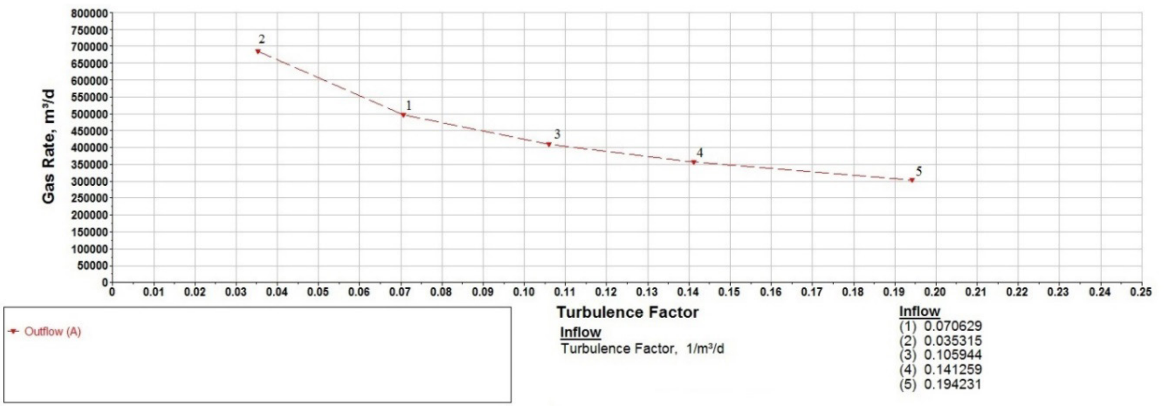

Fig. 14. Graph of gas flow vs. turbulence ratio

3.7. Evaluation of the sensitivity of a horizontal well to the water exponent

Analysing the diagram of pressure vs. gas flow rate as a function of the water exponent (Fig. 15), it may be stated that, for specific parameters of the reservoir and the BH3 well, the relations are as follows. Firstly, the higher the water exponent, the lower the gas flow rate. As regards the pink point on the reservoir productivity curve, it denotes the rate at which liquid and gas would start to destroy the wellbore on the basis of processes such as cavitation; however, since it has a very high value, it is not included in the diagram. The destruction rate decreases as the water exponent increases. It is also noticeable that for curves 3, 4, 5 there is a possibility of removing condensate and water, whereas for curves 1, 2 only condensate can be removed.

Analysing the curve of gas discharge depending on the water exponent (Fig. 16), it can be stated that in the range of the water exponent value 0.001 $m^3(l)/10^6m^3(g)$ to 5 $m^3(l)/10^6m^3(g)$ the curve of change of the discharge from the water exponent decreases slightly, which means that the gas discharge also decreases slightly. The further curve from the value of the water exponent of 5 $m^3(l)/10^6m^3(g)$ to 50 $m^3(l)/10^6m^3(g)$ decreases significantly, which means that the gas flow rate also decreases to a large extent. From the value of the water coefficient of 50 $m^3(l)/10^6m^3(g)$ to 100 $m^3(l)/10^6m^3(g)$, the curve stabilises, which means practically constant gas emission. This is due to the fact that the water is initially lifted point-wise upwards, which in the horizontal section merges into a shaft whose water mass is heavy and difficult to lift. Since such a large force is necessary, a greater depression in the reservoir is possible. This increases the output with less risk of water entering the well. Horizontal wells are therefore less sensitive to water inflow into the well. The last section of the curve of the change in flow rate from the water exponent from 100 $m^3(l)/10^6m^3(g)$ to 150 $m^3(l)/10^6m^3(g)$ decreases strongly, which means that the gas flow rate also decreases to a large extent.

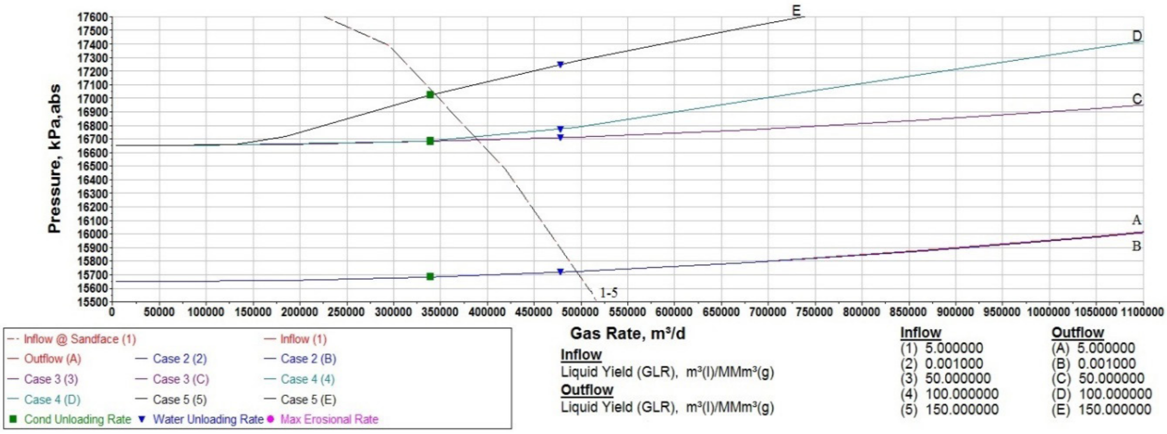

Fig. 15. Plot of pressure versus gas flow versus water exponent

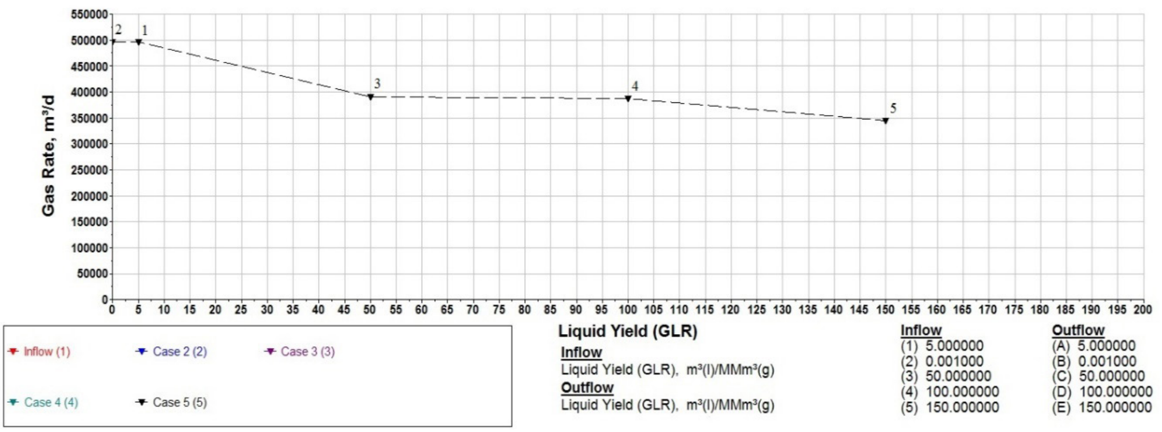

Fig. 16. Plot of pressure vs. gas flow vs. water exponent

4. Discussion

1. Horizontal wells are drilled into well-known structures which, after being drilled by vertical wells, provide a great deal of information on the spatial geometry or fracture structure of the reservoir, thus eliminating the risk of a possible unsealing of the reservoir structure through the unintentional drilling of a horizontal well into it.
2. The contact between the horizontal well and the reservoir is determined by the length of the horizontal well, which makes it possible to achieve a higher flow rate at the same depression. Horizontal wells are less sensitive to water inflow into the well because the pressure gradient is distributed over a certain length of the horizontal section.

3. An analysis of the course of the IPR curve (Fig. 5) as a function of the length of the horizontal section shows that the longer the horizontal section, the greater the gas flow rate. A significant increase in the gas discharge can be found in the length range from 10 m to 50 m. For greater values of the length of horizontal sections, the increase in output becomes weaker. It is important here that after exceeding the value of 440 m there is no visible increase in efficiency. It is also noticeable that for lengths of horizontal sections: 440, 200 (curves 1, 5) there is a possibility of carrying away condensate and water (Fig. 6).
4. From the analysis of the IPR curve (Fig. 7) on the pressure in the bed, it can be stated that the higher the pressure in the reservoir, the higher the gas output. A significant increase in gas output can be found in the range of reservoir pressure from 16,500 to 20,000 kPa. It is also noticeable that for the values of pressures in the reservoir: 18,000, 19,000, 20,000 (curves 1, 4, 5) there is a possibility of condensate and water extraction (Fig. 8).
5. From the analysis of the course of the IPR curve (Fig. 9) on the thickness of the deposit it can be stated that the greater the thickness, the greater the gas output. A significant increase of gas yield can be found in the thickness range from 10 m to 150 m. It can also be seen that for thickness values: 29, 50, 150 (curves 1, 4, 5), there is a possibility of condensate and water being carried away (Fig. 10).
6. From the analysis of the IPR curve (Fig. 11) on the average permeability of the deposit, it can be concluded that the higher the average permeability of the deposit, the higher the gas flow rate. A significant increase in the gas output can be found in the range of average reservoir permeability from 1 to 59 mD. For higher values of the vertical permeability of the reservoir, the increase in output increases more strongly. It can also be seen that for values of vertical bed permeability: 59, 100, 500 (curves 1, 4, 5), there is a possibility of condensate and water lift-off (Fig. 12).
7. The analysis of the IPR curve (Fig. 13) on the turbulence ratio shows that the higher the turbulence ratio, the lower the gas flow rate. A significant decrease in gas flow rate can be found in the range of turbulence ratio from 0.035315 $1/m^3/d$ to 0.070629 $1/m^3/d$. For higher values of turbulence coefficients, the decrease in output decreases more strongly. It is also evident that for the values of reservoir vertical permeability: 0.035315; 0.070629 (curves 1, 2), there is a possibility of condensate and water outflow (Fig. 14).
8. From the analysis of the course of the IPR curve (Fig. 15) from the water exponent it can be stated that the greater the water exponent, the smaller the gas output. A significant decrease in the gas yield can be found in the water exponent ranges from 5 $m^3(l)/10^6m^3(g)$ to 50 $m^3(l)/10^6m^3(g)$ and from 100 $m^3(l)/10^6m^3(g)$ to 150 $m^3(l)/10^6m^3(g)$. For values of the water exponent range from 50 $m^3(l)/10^6m^3(g)$ to 100 $m^3(l)/10^6m^3(g)$, the curve stabilises, which means practically constant gas output. This is due to the fact that the water is initially lifted upwards at a point, which in the horizontal section merges into a shaft whose water mass is heavy and difficult to lift. Since such a large force is necessary, a greater depression in the reservoir is possible. This increases the output with less risk of water entering the well. Horizontal wells are therefore less sensitive to water inflow into the well. It can also be seen that for a value of the water exponent of 0.001–5 (curves 2, 1), there is a possibility of condensate and water escaping (Fig. 16).

5. Conclusions

In conclusion, it is confirmed that the most important factors having the greatest influence on the efficiency of a horizontal well located in an underground gas storage facility are the following: reservoir pressure, thickness of the reservoir, length of the horizontal section, average permeability of the reservoir, turbulence coefficient and water exponent.

REFERENCES

[1] Gąska K., Hoszowski A., Gmiński Z., Kurek A.: *Monografia podziemnych magazynów gazu w Polsce*. Stowarzyszenie Inżynierów i Techników Przemysłu Naftowego i Gazowniczego Oddział Warszawa II, Warszawa 2012.

[2] Dokumentacja geologiczna złoża gazu ziemnego Bonikowo w kat. B – dodatek nr 1 – PGNiG Oddział Zielona Góra – rozliczenie zasobów, PGNiG SA w Warszawie. Zielona Góra, listopad 2009 [unpublished].

[3] Dokumentacja wynikowa odwiertu eksploatacyjnego Bonikowo 3H, PGNiG SA w Warszawie. Zielona Góra, kwiecień 2010 [unpublished].

[4] *Aktualizacja studium-wykonalności dla PMG Bonikowo na bazie częściowo sczerpanego złoża gazu ziemnego Bonikowo*, oprac. Zespół Rzeczoznawców, Grupa Terenowa z Zielonej Góry. Zielona Góra, styczeń 2006.
[5] Ahmed T.: *Reservoir Engineering Handbook*. Second edition, Gulf Professional Publishing 2007.
[6] Hagedorn A.R., Brown K.E.: *Experimental Study of Pressure Gradients Occurring During Continuous Two-Phase Flow in Small Diameter Vertical Conduits*. Journal of Petroleum Technology, Vol. 17, April 1965, pp. 475–484.
[7] *Materiały zebrane podczas praktyki dyplomowej dot. parametrów i zakresu pracy odwiertu horyzontalnego na podziemnym magazynie gazu*. Kraków [unpublished].
[8] Ahmed T.: *Equation of state and PVT analysis. Applications for Improved Reservoir Modeling*. Second edition, Gulf Professional Publishing 2007.
[9] Plume R.W.: *Ground-Water Conditions in Las Vegas Valley, Clark County, Nevada. Part 1: Hydrogelogic Framework*, *Clark County*. Department of Comprehensive Planning 1989.